

# Fabrication of Dye Sensitized Solar Cells with Different Natural Juices as Sensitizer on Polymer Substrates

S.D. Varathaseelan<sup>1</sup>

<sup>1</sup>Department of Science and Technology, Faculty of Science and Technology, Uva Wellassa University, Badulla, Sri Lanka

<sup>1</sup>[deepiseelan@yahoo.com](mailto:deepiseelan@yahoo.com)

---

**Abstract:** Typical solar cells contain glass substrate which make them fragile and heavy. Use of a plastic substrate on the other hand can make it very light and flexible. The use of natural pigments in photo-electro-chemical solar cells as a sensitizer is cost effective compare to that of ruthenium based metal centered dyes. Capability of dye extracted from different types of natural juices as a sensitizer in dye-sensitized solar cells with polymer substrates was studied. The solar cell performance of the natural dyes on TiO<sub>2</sub> films were studied by mean of the utilization as light harvesting electrodes in solid-state ITO/PEN/TiO<sub>2</sub>/naturalpigments/CuI/Pt-ITO/PEN cells. However, ruthenium based metal centered dyes exhibit much higher power conversion efficiency in dye-sensitized solar cells, due to excellent matching of band-gap with HUMO, LOMO levels of dye and charge transfer process.

**Keywords:** Dye-sensitized solar cells, photosensitization, quinonoidal, cole-cole plot, Nyquist diagram.

---

## I. INTRODUCTION

Dye sensitized solar cells (DSSC) belong to the third generation photovoltaic cells that convert visible light into electrical energy. In recent years, dye-sensitized systems have aroused much attention as a cheap alternative source for regenerative power sources. The dye-sensitization process on wide band gap semiconductors was investigated in 1960s. Since then rapid development of this field has to be seen. DSSCs made using conducting plastic substrate are flexible, thin, and light weight and enables them to use in commercial applications. A major problem of plastic substrate based DSSCs is their lower efficiency than that of glass substrate based DSSCs. Also there is another major problem in using plastic substrate in sintering of TiO<sub>2</sub> photo electrodes of DSSC which is usually done at high temperatures. Since the plastic substrates may not be able to heated up to 450°C like glass substrates as they could thermally unstable at high temperatures (450-550°C). The maximum temperature for plastic substrate (PEN Substrate) is about 150°C. So there is a need of an alternative technique for the TiO<sub>2</sub> deposition. The pressing of oxide layers for producing porous thin film was introduced by Hagfeldt et al. instead of high temperature preparation of nanostructured TiO<sub>2</sub> photo electrodes. They achieved an efficiency of 5.5% under 10mW/cm<sup>2</sup> irradiation and 3% efficiency under day time natural illumination. Several dyes are in use in manufacture of dye-sensitized solid state cells which are expensive. Use of natural pigments is a good solution for this and in nature, some fruits, flowers, leaves show various colors and contain several pigments that can be easily extracted and then employed in DSSCs. The aim of the present study was to investigate the photovoltaic performance of dye sensitized solar cell prepared with natural pomegranate, red-flesh dragon, prickly pear cactus and an unknown fruit juice sample as photosensitizer.

## II. METHODOLOGY

### 2.1 Deposition of nanocrystalline TiO<sub>2</sub> film on ITO/PEN substrates:

7 g of P-25 TiO<sub>2</sub> powder and 14mL of ethanol were placed in an agate ball milling jar with different size of agate balls. The mixture was milled with a speed of 250 rpm for 10 hours. TiO<sub>2</sub> slurry was coated on flexible ITO/PEN films (Peccell

Technologies, Inc., Japan) with the conductivity of  $13 \Omega\text{cm}^{-2}$  substrates by doctor blade technique.  $\text{TiO}_2$  coated ITO|PEN substrates were heated at  $150^\circ\text{C}$  for 30 min.  $\text{TiO}_2$  coated electrodes were transferred to a polyethylene envelope and sealed under a vacuum of  $10^{-1}$  Torr. Vacuum-sealed electrodes were pressed at room temperature using uniaxial pressing (Yankee hydraulic press, model no.YK20.v3).

## 2.2. Pigment coating procedure on $\text{TiO}_2$ film:

Different types of natural pigments were extracted by squeezing the ripe fruits. The juice was concentrated at  $60^\circ\text{C}$  in atmospheric condition. Pigment was coated on  $\text{TiO}_2$  electrodes as follows:  $\text{TiO}_2$  coated conducting plastic plates were kept immersed in a mixture of pigment solution. The temperature of the dye solution was maintained as  $40^\circ\text{C}$ . Pigment amount on  $\text{TiO}_2$  electrodes was controlled by varying the immersion time in the dye solution.

## 2.3. Assembling of the cell:

### 2.3.1. Preparation of Pt coated electrodes:

10 mM  $\text{H}_2\text{PtCl}_6$  in isopropanol solution was prepared. One drop of this solution was put onto the conductive side of ITO|PEN electrode and allows drying. ITO counter electrode (active side up) was inserted into ceramic tube, gradually heated up to  $400^\circ\text{C}$ , left for 15 min., allowed the electrode to cool. A hole with a diameter of 1 mm was made on the Pt coated ITO electrode.

### 2.3.2. Preparation of solar cell with plastic substrates:

Dyes coated films were rinsed with ethanol and dried at room temperature. Dye-sensitized solar cell devices were fabricated by attaching a Pt|ITO|PEN to the dye-coated  $\text{TiO}_2$ |ITO|PEN electrode. The electrolyte that was composed of 0.04 M  $\text{I}_2$ , 0.4M 4tert-butylpyridine, 0.4M lithium iodide, 0.3M N-methylbenzimidazole in acetonitrile and 3-methoxypropionitrile by volume 1:1 was filled in between the electrodes by the capillary action.

## 2.4. Measurements:

Absorption spectra of dye solutions and dye coated  $\text{TiO}_2$  films were measured by using UV-VIS-NIR spectrometer (Jasco V-570). Morphology of the cell was studied using scanning electron microscope. Photo-effects of the cell were studied by illuminating the cell through  $\text{TiO}_2$  layer. The variation of photocurrent of the cell with the wavelength was measured using monochromator (Jasco) coupled with single-phased lock-in amplifier (NF Instrument-5600 A), under constant photon energy illumination mode. Current-voltage characteristics were recorded with a solar simulator (Wacom) coupled with semiconductor parameter analyser (Hewlett Packard HP 4145B), under AM 1.5 condition. Scan speed was maintained at  $0.01 \text{ Vmin}^{-1}$ . The interfacial electrical properties of the cells were studied natural bias under a three-electrode configuration with the same electrolyte, by using a multi-channelled potentiostat (Princeton Applied Research) coupled with a computer. The charge transfer resistance at the electrolyte–electrode interface was evaluated from E Clab software.

## III. RESULTS AND DISCUSSION

These  $\text{TiO}_2$  electrodes are composed with three components, namely (a) dense  $\text{TiO}_2$  layer, (b) nano-crystalline  $\text{TiO}_2$  layer and (c) meso-porous  $\text{TiO}_2$  layer.

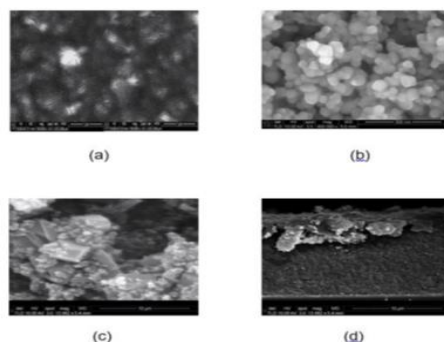


Figure 3.1 Morphology of  $\text{TiO}_2$  electrodes a) dense  $\text{TiO}_2$  layer, (b) nano-crystalline  $\text{TiO}_2$  layer and (c) microcrystalline  $\text{TiO}_2$  layer and (d) cross section of the electrode.

The morphology of each TiO<sub>2</sub> layer is shown in Fig. 3.1. These three layers can be easily distinguished by the morphological appearances of the layers. The cross-sectional image of the electrode is shown in the same figure (image d).

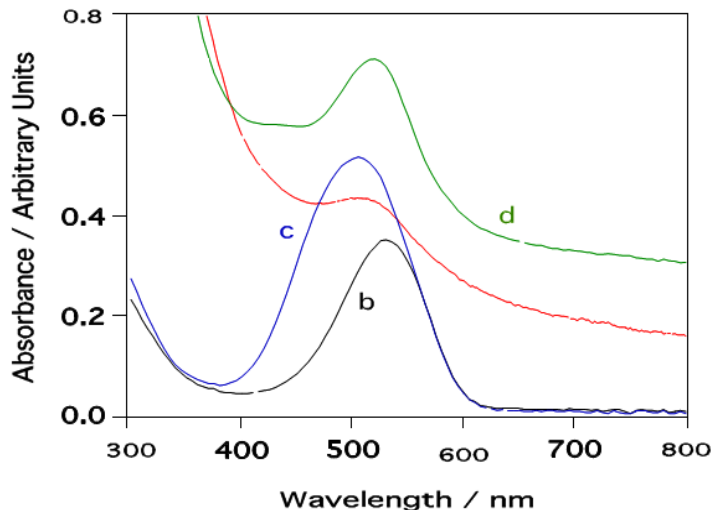


Figure 3.2 Absorption spectrum of natural fruit juice of (a) pomegranate (b) red-flesh dragon (c) prickly pear cactus and (d) unknown fruit juice

Absorption spectrum of natural fruit juice (a) pomegranate (b) red-flesh dragon (c) prickly pear cactus and (d) unknown is shown in Fig. 3.2. These fruit juices absorb different regions of visible light due structural differences of their pigment particles.

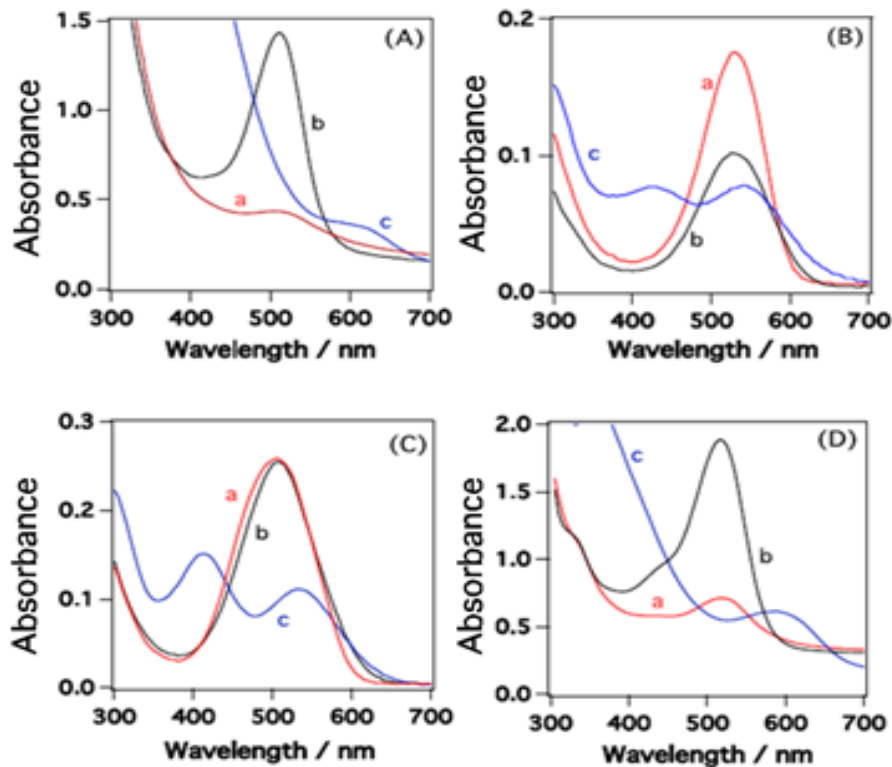


Figure 3.3 Absorption properties, (a) natural, (b) acidic and (c) basic solutions of fruit juices for (A) pomegranate, (B) red-fleshed dragon, (C) prickly pear cactus, and (D) unknown

Absorption properties of fruit juices (A) pomegranate, (B) red-fleshed dragon, (C) prickly pear cactus and (D) unknown were studied under natural, acidic and basic media (With pH 6.3, 3.1 and 8.7 respectively) and results are shown in Fig. 3.3. Natural pomegranate juice absorbs visible light with a maximum at 510 nm (curve a in Fig. 3.3(A)). However, addition of several drops of HCl to the natural juice enhanced the intensity of the absorption maximum by several fractions (hyperchromic shift) (curve b in Fig. 3.3(A)). However, a bathchromic shift with a magnitude of 100 nm was observed in the absorption spectrum of basic pomegranate (After the addition of NaOH) juice compare to that of the natural juice. Absorption spectrum for natural juice of red-flesh dragon fruit (a) natural (b) acidify and (c) basic juices is shown in Fig. 3.3(B). A significant reduction in absorption properties (hypochromic shift) of acidify medium was observed. This result is contrast with the result observed by adding acid in to pomegranate juice (curves b in Fig. 3.3 (A&B)). No significant change was observed in the absorption by adding acid into prickly pear cactus juice (curves a & b in Fig. 3.3 (C)). A shift and split with a reduction in the intensity in the absorption band were observed by adding base in to red-flesh dragon, prickly pear cactus fruit juice (curves c in Fig. 3.3 (B&C)). Unknown fruit juice also behaves as a similar manner to that of pomegranate juice, with the acid and base treatments

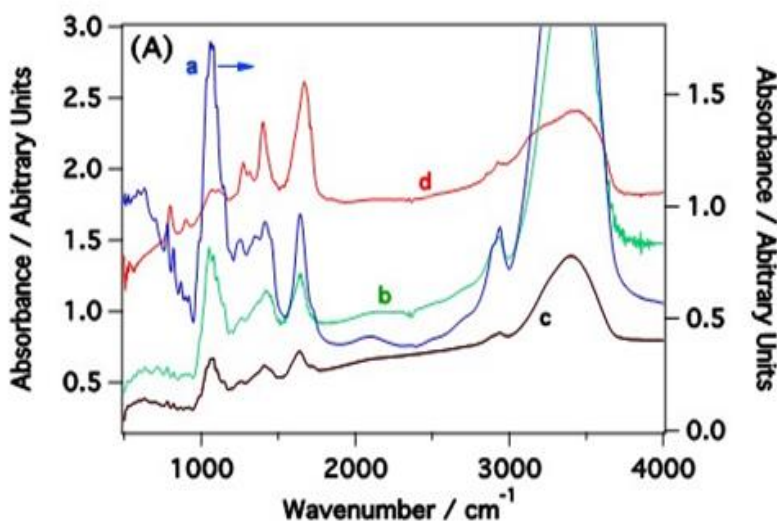


Figure 3.4 FTIR spectrum of natural fruit juice (a) pomegranate (b) red-flesh dragon fruit (c) prickly pear cactus and (d) unknown

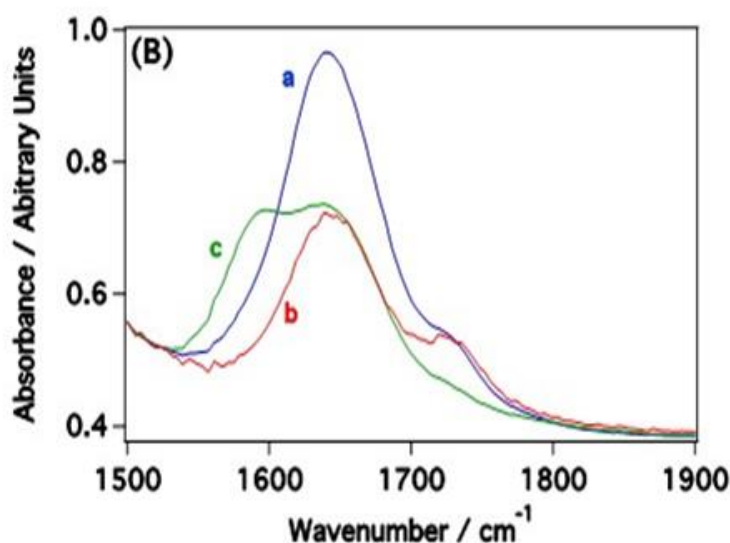
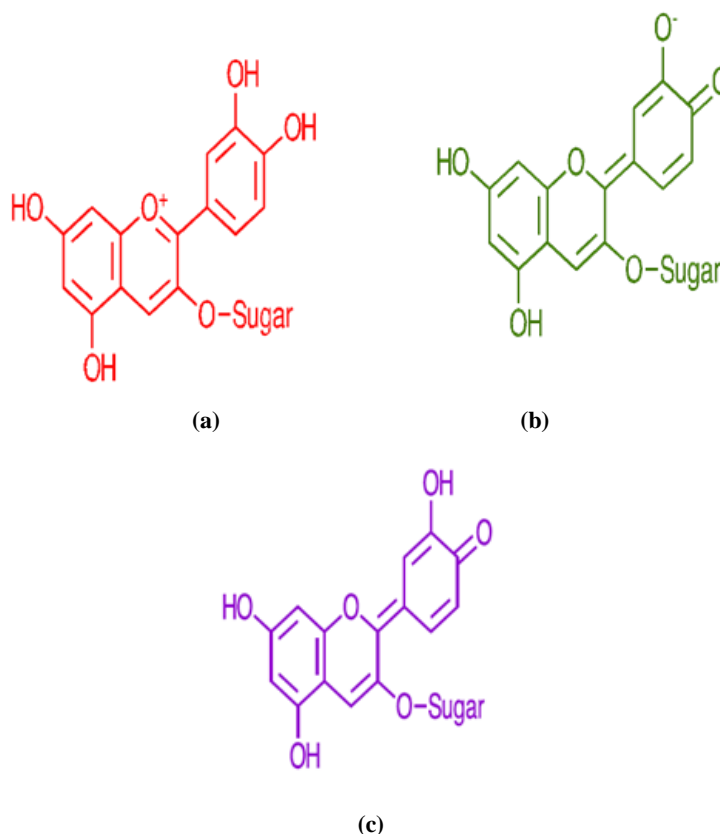


Figure 3.5 FTIR spectra for (a) acid, (b) natural and (c) based added pomegranate juice

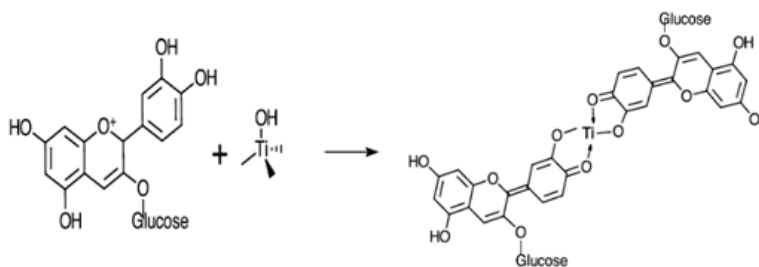
FTIR spectra of natural fruit juice (a) pomegranate (b) red-flesh dragon fruit (c) prickly pear cactus and (d) unknown are shown in Fig. 3.4. Though intensity of characteristics peaks varies (depends on the concentration of the fruit samples), characteristic peaks were shown at 3400, 2930, 1639 and 1053  $\text{cm}^{-1}$  in FTIR spectra, for all the samples. These peaks can be assigned to; stretching of OH groups, aliphatic hydrogen, carbonyl groups and C-O-C bond, respectively [10, 11]. FTIR spectra for acid and base added juice samples were also studied. For an example, FTIR spectra for (a) acid, (b) natural and (c) base added pomegranate juice are shown in Fig. 3.5. A clear splitting of the peak at 1639  $\text{cm}^{-1}$  (curve c in Fig. 3.5) was observed for base added fruit juice. No detectable deviation on the FTIR spectrum was observed for acid added juice (curve a in Fig. 3.5) compare to that of natural juice (curve b in Fig. 3.5). It is known that dye molecules behave in different manner in different environments, probably due to enforcement of Van der Waals interaction between dye molecules and solvents depending on their polarity [9].

The composition and structure of red-flesh dragon, prickly pear cactus and unknown is not known, As reported elsewhere, pomegranate fruit juice contains several anthocyanins, and other phenolic compounds [10]. Cyanadin-3-glucoside is the most known compound in pomegranate fruit juice. These molecules mainly composed from benzopyril group and phenolic group [11]. Colour of the compound strongly depends on the numbers of substituents in phenolic rings [12]. Molecular structure of (a) flavylum form (acidify), (b) quinonoidal form (natural) and (c) basic forms of cyanadin-3-glucoside are shown in scheme 1 [13].



**Scheme1. Structure of (a) acidified, (b) natural and (c) basic pomegranate juice**

We have made an attempt to coat acidified, natural and basic fruit juices on  $\text{TiO}_2$  electrodes. Degree of absorption of red-flesh dragon, prickly pear cactus and unknown fruit juice on  $\text{TiO}_2$  electrodes was feeble except pomegranate juice. Acidified and natural pomegranate juices coated  $\text{TiO}_2$  electrodes exhibited purple colour and basic pomegranate juice coated  $\text{TiO}_2$  electrodes exhibited green colour for naked eye. Chelating of flavylum form of cyanadin-3-glucoside with  $\text{TiO}_2$  results quinonoidal form of cyanadin-3-glucoside [13]. Recently, it has been confirmed that cyanadin-3-glucoside bonds with metal ions via bidentately in the pH range of 1-3 [14]. Therefore, following mechanism for chelation of cyanadin-3-glucoside with  $\text{TiO}_2$  in acidic medium can be proposed.



Scheme 2. Chelation of Quinonodal form of cyanadin-3-glucoside with TiO<sub>2</sub>

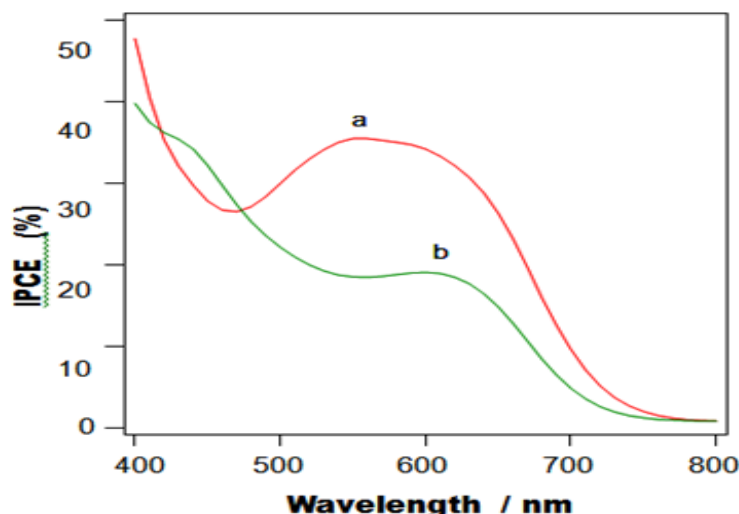


Figure 3.6 IPCE Spectrum for the cells prepared by using (a) acidified and (b) basic pomegranate fruits juice.

The maximum IPCE (incident photon to current conversion efficiency) of 38% was observed for the cells prepared by using acidified pomegranate fruits juice at the wavelength of 570 nm (curve a, Fig. 3.6). IPCE action spectrum of the cell fabricated by using a basic pomegranate dye coated TiO<sub>2</sub> electrode is shown as curve b in Fig. 3.6. Clear red shift with a magnitude of 50-60 nm was observed in the absorption spectrum of pomegranate juice (acid or natural) coated TiO<sub>2</sub> electrode compare to that of the basic pomegranate juice coated TiO<sub>2</sub> electrode. The maximum IPCE of 19% was observed for the cells prepared by using basic pomegranate fruits juice at the wavelength of 610 nm (curve b, Fig. 3.6).

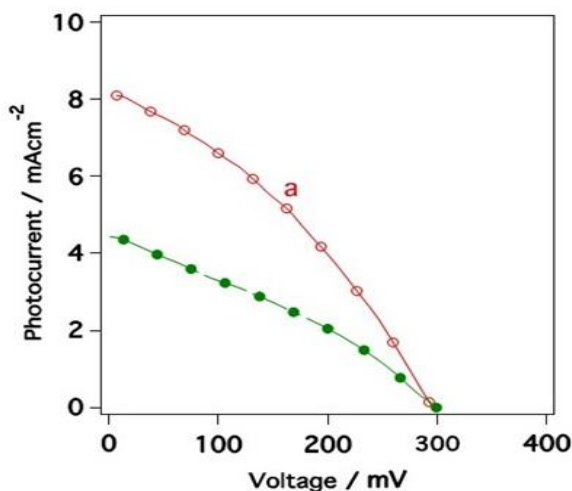


Figure 3.7 Current–voltage characteristics of TiO<sub>2</sub>|pomegranate pigments|electrolyte cell.

Current–voltage characteristics of TiO<sub>2</sub>|pomegranate pigments|electrolyte cell is shown in Fig. 3.7. We have observed a maximum photocurrent density of  $8 \pm 0.5 \text{ mA cm}^{-2}$  and a photovoltage of  $300 \pm 40 \text{ mV}$  with a higher reproducibility for TiO<sub>2</sub>|pomegranate pigments|electrolyte cells and results are compared with the cell prepared with Ru-metal centered dye with same configuration. Approximately two times greater photo-performance is observed for Ru-metal complex based photovoltaic cells compare to that of TiO<sub>2</sub>|pomegranate pigment based cells [15-17].

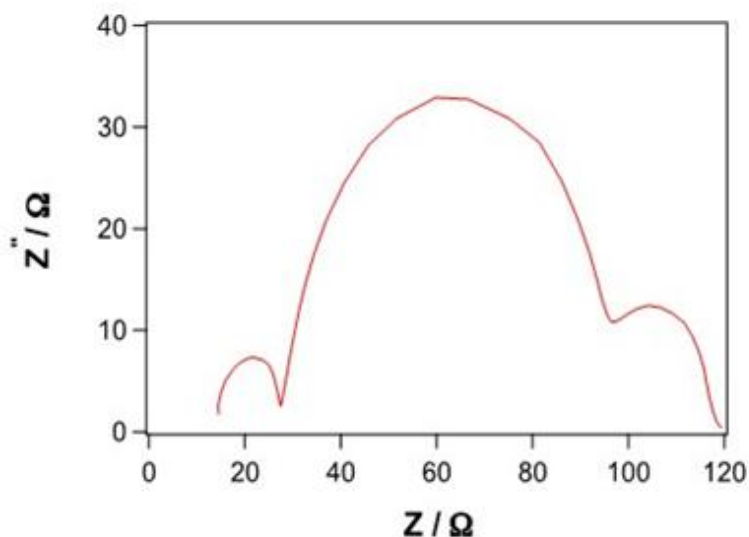


Figure 3.8 Nyquist diagram of TiO<sub>2</sub>|pomegranate pigments|electrolyte cell.

Fig. 3.8 represents the Nyquist diagram of pomegranate pigment coated electrode. A typical Nyquist diagram for glass based DSSCs normally features three semicircles. The semicircle corresponding to the higher range of frequencies (the left semicircle, with diameter R<sub>1</sub>), the middle range of frequencies (the middle semicircle, diameter R<sub>2</sub>) and the lower range of frequencies (the right semicircle, diameter R<sub>3</sub>) represent I<sub>3</sub><sup>-</sup> transport in the electrolyte, electron recombination at the TiO<sub>2</sub>|electrolyte interface together with electron transport in the TiO<sub>2</sub> network and the redox reaction at the platinum counter electrode, respectively [18]. The high frequency intercept with the real axis is the ohmic resistance (R<sub>0</sub>) and is related with the sheet resistance of the substrate of the working electrode. Values of R<sub>0</sub> – R<sub>3</sub> were evaluated as 14, 10, 35 and 18 Ω from the ECLab software.

#### IV. CONCLUSION

Photo-performance of four different natural juices sensitized solar cells was studied. Degree of absorption of red flesh dragon, prickly pear cactus and unknown fruit juice on TiO<sub>2</sub> electrodes was feeble except pomegranate juice. We have observed a maximum photocurrent density of  $8 \pm 0.5 \text{ mA cm}^{-2}$  and a photovoltage of  $300 \pm 40 \text{ mV}$  with a higher reproducibility for TiO<sub>2</sub>|pomegranate pigments|electrolyte cells. So we can say that Ru-metal complex based photovoltaic cells give two times greater photo-performance when compared with pomegranate juice based cells.

#### REFERENCES

- [1] Botkin D. B., Keller E. A (2009). Environmental science- earth as a living planet, 7th edition, pp 392.
- [2] Jasim K.E. (2003) Dye sensitized solar cells-working principles, Challenges and opportunities.
- [3] Yamaguchi T., Tobe N., Arakawa H.(2013) et al, Highly efficient plastic-substrate dye – sensitized solar cells with validated conversion efficiency of 7.6%
- [4] Peng Y., Liu JZ, Wang K, Cheng YB (2011) Influence of parameters of cold isostatic pressing on TiO<sub>2</sub> films for flexible dye- sensitized solar cells. Int. J. Photon energy, Article ID 410352, 7 pages.
- [5] Carpel U.T.E. (2003) Characterization of Organic Dyes for Solid State Dye Sensitized Solar Cells.

**International Journal of Novel Research in Engineering and Science**

Vol. 4, Issue 2, pp: (10-17), Month: September 2017 - February 2018, Available at: [www.noveltyjournals.com](http://www.noveltyjournals.com)

- [6] Weerasinghe HC, Sirimanne PM, Simon GP, Cheng YB (2012) Cold isostatic pressing technique for producing high efficient flexible dye sensitized solar cell on plastic substrates. *Progress in Photovoltaics* 20(3): 321-332.
- [7] Weerasinghe H.C., Sirimanne P.M., Simon G.P., Cheng Y. (2011) Fabrication of efficient solar cells on plastic substrates using binder-free ball milled titania slurries.
- [8] O. Dangles, M. Elhabiri, R. Brouillard (2012) *J. Chem. Soc., Perkin Trans.* 2587
- [9] B. O'Regan, M. Gratzel. (1994) A low-cost high-efficiency solar cell based on dye-sensitized colloidal TiO<sub>2</sub> films, *Nature*, 353 737 – 740.
- [10] Seigo Ito, (2013) Investigation of dyes for dye-sensitized solar cells: Ruthenium- complex dyes, metal-free dyes, metal – complex porphyrin dyes and natural dyes.
- [11] Zakerhamidi MS, Ghanadzadeh A, Moghadam M (2012) Solvent effects on the UV/visible absorption spectra of some aminoazobenzene dyes. *Chem Sci Trans.*,1 (1): 1-8.